Senescent fibroblast-derived Chemerin promotes squamous cell carcinoma migration

Supplementary Materials

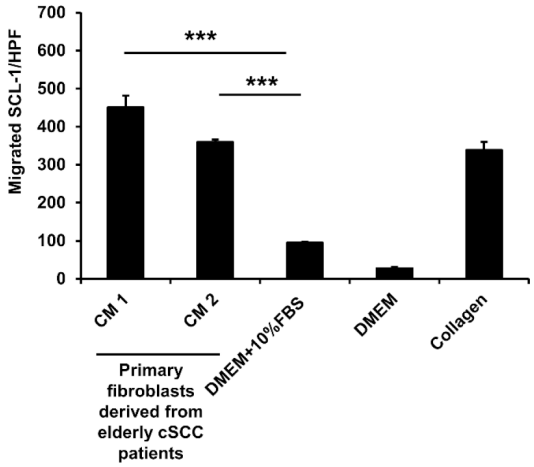

Supplementary Figure S1: Migration of SCL-1 cells in response to conditioned media derived from intrinsically aged primary fibroblast of cSCC patients. Conditioned media (CM) was prepared from two different cSCC-associated stromal fibroblasts from elderly cSCC patients at an age of 88 years and 92 years (F-SCC3 and F-SCC1160524) to induce the migration of SCL-1 cells using the Transwell® chamber migration assay. DMEM containing 10% FBS and collagen type I at a concentration of 50 µg/ml served as positive controls. DMEM served as a negative control. Displayed are the result of migration assay using two different passages of primary fibroblast F-SCC1160524 (labeled as CM1 and CM2). The results indicate that CM of primary fibroblasts of elderly cSCC patients significantly enhance the migration of SCL-1 compared to DMEM containing 10% FBS. Data are shown as mean ± S.D with $n = 3$ replicate wells; ***$p < 0.001$ calculated by unpaired student t-test between CM-treated and DMEM-10% FBS treated groups; HPF= ×100 magnification. Similar results were obtained using primary aged stromal fibroblast F-SCC3 (CM1 = 351 ± 43 cells/HPF and CM2 = 333 ± 52 cells/HPF).

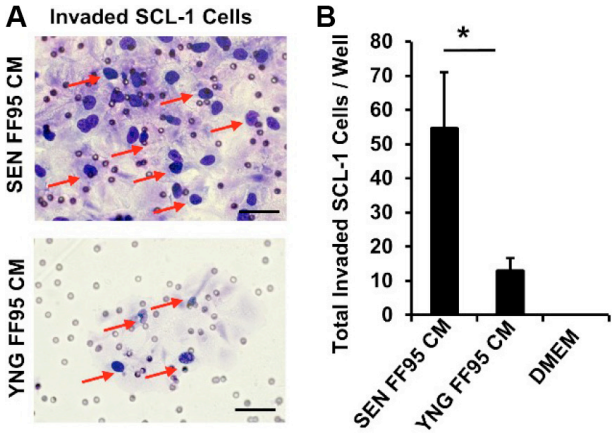

Supplementary Figure S2: Secretome of senescent fibroblasts enhances the invasion of SCL-1 tumor cells. Cell invasion assay was performed similar to migration assay apart from coating a layer of BD Matrigel™ was coated (100 µl/well) onto the upper filter of Transwell® chambers 4 hours prior to the experiment. The lower compartments of the chambers were loaded with CM of senescent and young FF95 fibroblasts and incubated for 14 h at 37°C. DMEM served as a control to monitor random invasion. Cells stained purple by Diff-Quick staining kit and counted under light microscopy at ×100 magnification (**A**) Representative images (×200 magnification, scale bars = 50 µm) showing invaded SCL-1 cells (pointed with red arrows) at the downside of the membrane in response to CM from senescent vs. young fibroblasts. (**B**) Quantifications of cell invasion proved that senescent FF95 CM increased the invasion of SCL-1 tumor cells. Graph is a representative of three independent experiment. *$p < 0.05$ calculated by unpaired student t-test; HPF= ×100 magnification.

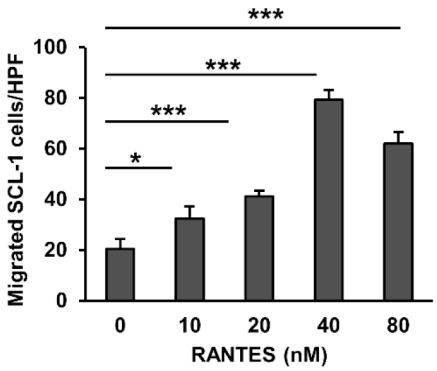

Supplementary Figure S3: Effect of rh RANTES/CCL5 chemokine on SCL-1 cell migration. Effect of rh RANTES/CCL5 chemokine on SCL-1 cell migration. The graph depicts the quantification of migrated SCL-1 cells after 14 h treatment with increased concentration of rh RANTES using Transwell chamber migration assay. Results are expressed as the mean number of migrated cells ± S.D for $n = 4$ replicate wells (HPF = ×100 magnification). The results are representative of one of three independent experiments. *$p < 0.05$, ** $p < 0.01$ and ***$p < 0.001$ calculated by Bonferroni post hoc test after ANOVA.

Up-regulated Genes in SCL-1 cells compared to Keratinocytes

Gene Symbol	Ref Seq	Fold Regulation	P-value
CCRL2	NM_003965	183,4063	0,000004
CCR10	NM_016602	32,7253	0,000022
CXCR6	NM_006564	8,3072	0,001035
CCL22	NM_002990	4,618	0,003824
CXCL16	NM_022059	4,1799	0,00634
CKLF	NM_181641	4,0689	0,000011
CCL5	NM_002985	3,0436	0,000935
CMTM4	NM_178818	2,7618	0,000089
CX3CL1	NM_002996	2,2006	0,00046
CCR1	NM_001295	2,1054	0,042869
CCR3	NM_001837	1,9931	0,011117

Down-regulated Genes in SCL-1 cells compared to Keratinocytes

Gene Symbol	Ref Seq	Fold Regulation	P-value
CCL2	NM_002982	-820,8649	0,003518
CXCL14	NM_004887	-719,5582	0,000001
SLIT2	NM_004787	-317,4681	0,000016
CXCL5	NM_002994	-286,6343	0,000001
CXCR7	NM_020311	-180,4974	0,000004
CMKLR1	NM_004072	-168,4801	0,004805
PPBP	NM_002704	-164,4419	0,000035
CXCL10	NM_001565	-131,4194	0,000009
TNF	NM_000594	-110,1837	0
CXCL12	NM_000609	-89,4371	0,000124
CXCR1	NM_000634	-40,5829	0,000044
CXCL11	NM_005409	-31,768	0
DARC	NM_002036	-15,4736	0,000054
CCL20	NM_004591	-12,9296	0,000008
CXCL6	NM_002993	-12,9251	0,000395
CCL7	NM_006273	-8,3245	0,000008
PF4V1	NM_002620	-5,6034	0,049416
CXCL3	NM_002090	-5,5716	0,000001
IL8	NM_000584	-5,5518	0,000073
FPR1	NM_002029	-5,0442	0,000186
CCL19	NM_006274	-4,8872	0,001296
CCR2	NM_00112339 6	-4,8617	0,016555
CCR6	NM_004367	-4,544	0,013578
CCL11	NM_002986	-3,4654	0,026887
CXCL9	NM_002416	-3,2673	0,010818
CCBP2	NM_001296	-3,2286	0,002358
TYMP	NM_001953	-3,1654	0,00018
CXCL1	NM_001511	-3,086	0
CCL27	NM_006664	-2,3925	0,002334
CXCL2	NM_002089	-2,0467	0,00002
CCR5	NM_000579	-1,8123	n.s.
CCR4	NM_005508	-1,5679	0,041545
CXCR2	NM_001557	-1,4416	0,010917

Supplementary Figure S4: Expression profile of chemokine and chemokine receptors in SCL-1 cell line compared to normal keratinocytes. Heat maps illustrate differentially regulated chemokine and chemokine receptor genes in SCL-1 cell line compared with normal keratinocytes. Red and green colors represent upregulation and down-regulation, respectively. Tables indicate fold changes and significance levels in mRNA expression of chemokines and their receptors in SCL-1 cell line compared to normal keratinocytes. The expression level of selected chemokine receptors (shown with boxes), which were relevant to SASP-induced migration, was further assessed using qRT-PCR analysis. Of note, CCRL2 has the highest fold regulation among other chemokine receptors expressed in SCL-1 tumor cells.

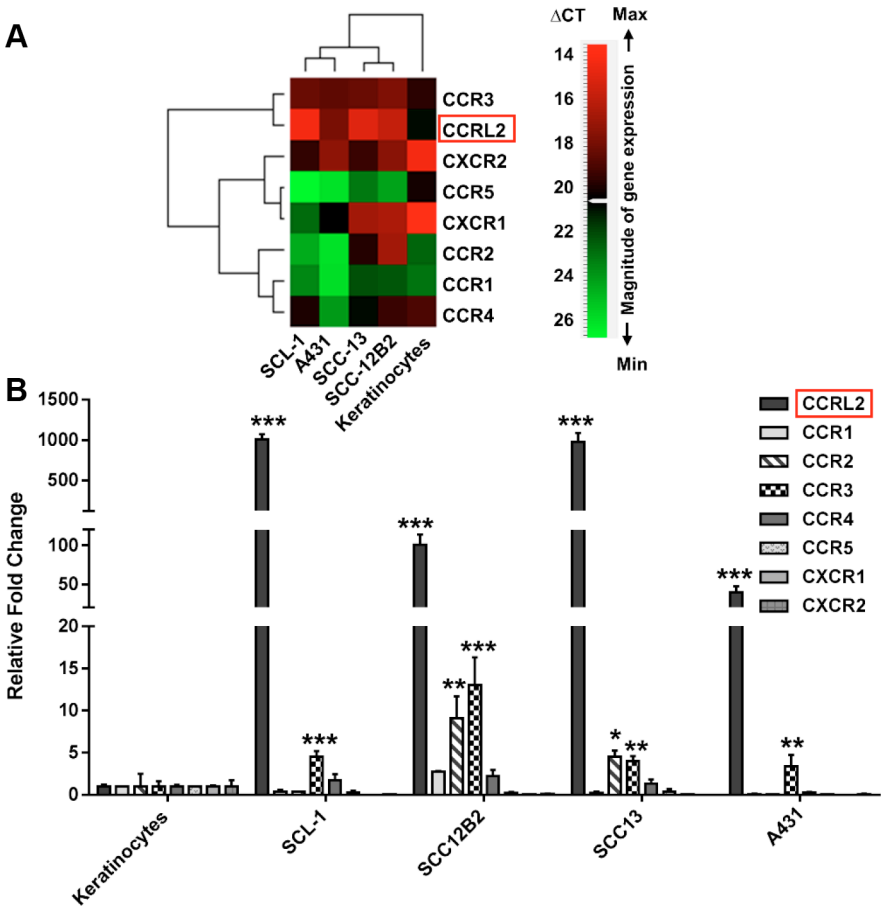

Supplementary Figure S5: Expression pattern of selected chemokine receptors in cSCC cell lines vs. normal keratinocytes. Quantitative RT–PCR for selected chemokine receptors was performed to validate the RT2 Profiler PCR data in keratinocytes vs. cSCC cell lines (SCL-1, SCC12B2, SCC-13 and A431) (**A**) Heat map illustrating differentially expressed chemokine receptors. Signal intensities were averaged between biological replicates of three independent experiments and normalized to the averaged signal from biological replicates of normal keratinocytes. Green indicates downregulation (lower delta Ct values) and red upregulation (higher delta Ct values). (**B**) Graph represents the relative fold changes in mRNA expression normalized to the average expression level in keratinocytes. The qRT–PCR experiment was performed independently three times using samples prepared separately from the PCR array experiment. Data are shown as mean ± S.D for one of three independent experiments with $n = 3$; *$p < 0.05$, **$p < 0.01$ and ***$p < 0.001$ calculated by Bonferroni post hoc test after ANOVA shown for upregulated genes in cSCC cell lines as compared to normal keratinocytes.

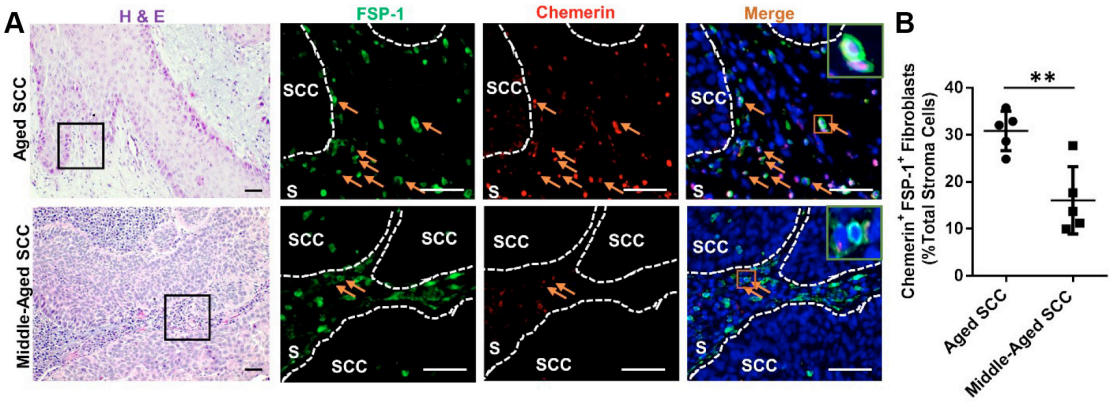

Supplementary Figure S6: Immunofluorescence staining of Chemerin and the fibroblast marker FSP-1 in paraffin-embedded skin sections of cSCC patient biopsies. (**A**) Representative microphotographs of skin sections derived from an aged cSCC patient (83 years), and relatively younger patient (61 years), stained for the fibroblast marker FSP-1 (green), Chemerin (red), and with DAPI for nuclei (blue). Scale bars = 50 µm at × 400 magnification; Dashed lines delineate SCC from stroma (S). Orange arrows point to the Chemerin positive fibroblasts, indicating higher numbers of Chemerin expressing fibroblasts in sections from a very old cSCC patient compared to middle-aged cSCC patient. (**B**) Graph representing the quantification of percentage of FSP-1 and Chemerin double-positive cells normalized to the total number of nuclei in the tumor stroma of cSCC patients at different age groups (80 ± 5 years, $n = 5$ cSCC patients) and middle-aged (54 ± 5 years, $n = 5$ donors). Unpaired student t-test revealed statistical significant differences (**$p < 0.01$) between the two groups.

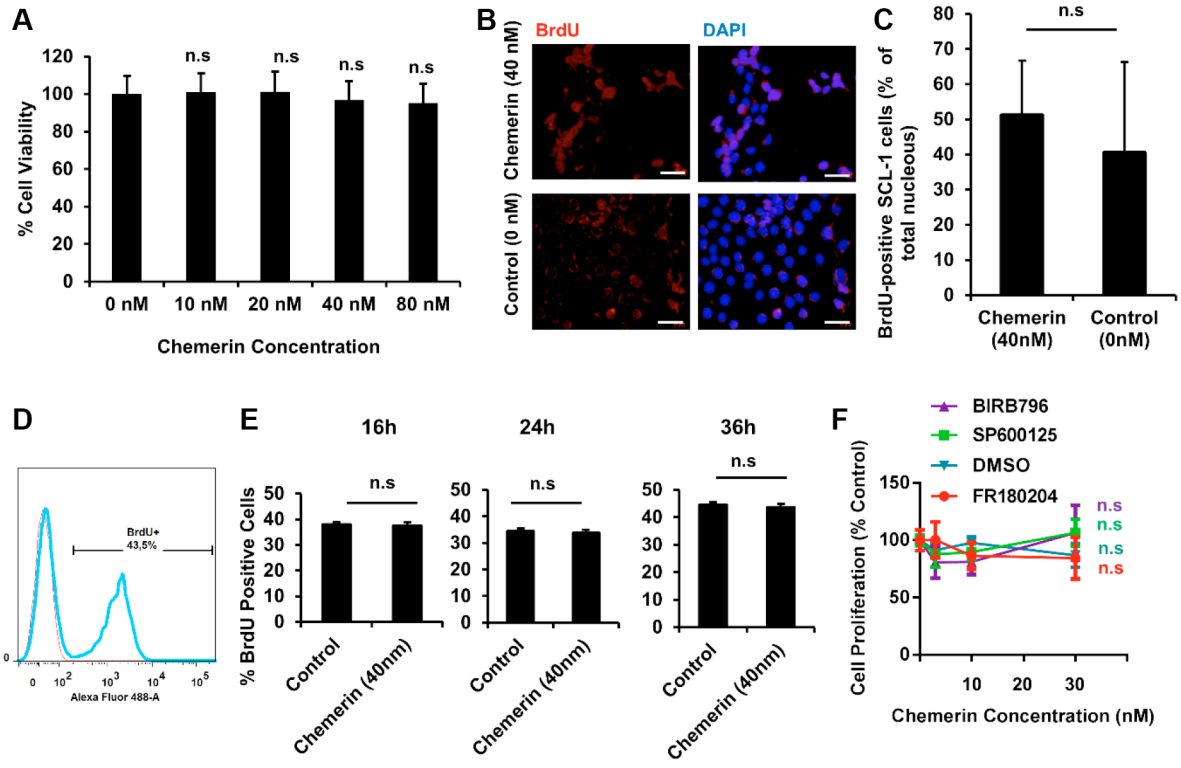

Supplementary Figure S7: SCL-1 cell proliferation/survival analysis in response to rh Chemerin and MAPK inhibitors using MTT and BrdU assays. (**A**) Graph demonstrating that Chemerin has no significant effect on the percentage of metabolically active living cells as defined by MTT assay, indicating that Chemerin probably does not induce pathways involved in cell proliferation, viability and metabolism. Data are shown as the mean percentage ± S.E.M live metabolically active SCL-1 cells treated with Chemerin compared to untreated cells (n = 5 independent experiments; n.s. = non. Significant as indicated with ANOVA). (**B**–**E**) To assess the effect of Chemerin on cell proliferation, SCL-1 cells were cultured with (or without) Chemerin for the indicated times, pulse labeled with BrdU for 2 hours, harvested and fixed. DNA synthesis was assessed by staining with an antibody to BrdU, and measured by (B and C) immunofluorescence microscopy, and (D and E) flow cytometry analysis. (B) Representative pictures of immunofluorescence staining showing the expression of BrdU-incorporated SCL-1 cells after 24 hour treatment with 40 nM Chemerin compared with untreated controls. Cells were stained with anti- BrdU specific mAb in red. Nuclei were DAPI-counterstained in blue. Scale bars = 50 µm. (**C**) Quantification of BrdU-incorporated SCL-1 nuclei in Chemerin-treated and untreated SCL-1 cells. Results are the mean ± S.D. of three biological replicates. n.s.= non-significant as calculated with unpaired student t-test. (D) Histogram representative of flow cytometric analysis showing the percentage of BrdU-positive SCL-1 cells as defined by mean fluorescent intensity of anti-BrdU antibody conjugated with Alexa-fluor488. The solid blue line depicts BrdU expression and red histogram is negative control with no DNA-incorporation of BrdU. (E) Bar charts represent one of three independent experiments demonstrating the mean percentage ± S.D. of BrdU incorporated SCL-1 cells, showing no statistically significant difference as analyzed by unpaired student t-test. (**F**) Graph demonstrating the cytotoxicity of MAPK inhibitors on SCL-1 cells as defined by MTT assay. Cytotoxicity was calculated as the percentage of metabolically active living cells treated with different agents compared with cells treated with DMSO as a vehicle control. None of the inhibitors has cytotoxic effect on SCL-1 cells as computed by linear regression analysis. Data points are mean ± S.D for five samples per MAPK inhibitor. The experiment was repeated five times. $p < 0.05$, $^{**}p < 0.01$ and $^{***}p < 0.001$.

Supplementary Table S1: List of cSCC and normal skin samples used for immunostaining

Sample Nr.	Tissue type/ Diagnisis	Gender	Age	Location	Broder's classification
1	cSCC	F	90	Hairy head skin	Moderately-differentiated
2	cSCC	F	87	Cervical spine	Well-differentiated
3	cSCC	M	85	Temple	Moderately-differentiated
4	cSCC	M	83	Lower lip	Moderately-differentiated
5	cSCC	M	83	Forehead	Moderately-differentiated
6	cSCC	M	83	Hand	Moderately-differentiated
7	cSCC	F	75	Nose	Moderately-differentiated
8	cSCC	M	75	Nose	Poorly-differentiated
9	cSCC	M	74	Lower arm	Well-differentiated
10	cSCC	M	73	Hairy head skin	Well-differentiated
11	cSCC	F	72	Forehead	Well-differentiated
12	cSCC	F	61	Nose	Moderately-differentiated
13	cSCC	F	56	Cheek	Well-differentiated
14	cSCC	M	52	Cheek	Moderately-differentiated
15	cSCC	M	50	In front of ear	Well-differentiated
16	cSCC	M	50	In front of ear	Moderately-differentiated
17	Normal Skin	F	91	Back	
18	Normal Skin	M	89	Left occipital	
19	Normal Skin	M	82	Back	
20	Normal Skin	M	82	Sternal	
21	Normal Skin	M	79	Back	
22	Normal Skin	M	79	Left shoulder	
23	Normal Skin	M	77	Back	
24	Normal Skin	F	74	Right neck	
25	Normal Skin	F	74	Lower arm	
26	Normal Skin	M	73	Back	
27	Normal Skin	F	72	Left shoulder	
28	Normal Skin	F	72	Back	
29	Normal Skin	M	71	Ear	
30	Normal Skin	M	70	Back	
31	Normal Skin	M	47	Back	
32	Normal Skin	M	42	Back	
33	Normal Skin	M	36	Hairy head skin	
34	Normal Skin	F	31	Knee	
35	Normal Skin	F	24	Back	
36	Normal Skin	F	24	Back	
37	Normal Skin	M	23	Schoulder	
38	Normal Skin	M	19	Lower left thigh	
39	Normal Skin	F	18	Back	
40	Normal Skin	F	16	Armpit	
41	Normal Skin	M	16	Left paravertebral	
42	Normal Skin	M	16	Back	
43	Normal Skin	F	16	Buttocks	
44	Normal Skin	F	16	Breast skin	
45	Normal Skin	F	15	Upper stomach skin	
46	Normal Skin	F	15	Forhead	
47	Normal Skin	F	13	Back	
48	Normal Skin	M	13	Left foot sole	
49	Normal Skin	F	9	Back	
50	Normal Skin	M	5	Back	

Supplementary Table S2: List of primers used for qRT-PCR purchased from qiagen (hilden, germany)

Gene	Product Name	CAT No. C
Actin	QuantiTect Primer Assay Hs_ACTB_2_SG	QT01680476
CCL5	QuantiTect Primer Assay Hs_CCL5_1_SG	QT00090083
CCR1	QuantiTect Primer Assay Hs_CCR1_1_SG	QT00047740
CCR2	QuantiTect Primer Assay Hs_CCR2_1_SG	QT00000224
CCR3	QuantiTect Primer Assay Hs_CCR3_2_SG	QT02423596
CCR4	QuantiTect Primer Assay Hs_CCR4_1_SG	QT00208950
CCR5	QuantiTect Primer Assay Hs_CCR5_1_SG	QT00998802
CCRL2	QuantiTect Primer Assay Hs_CCRL2_1_SG	QT00225988
CMKLR1 va. 1	QuantiTect Primer Assay Hs_CMKLR1_va.1_SG	QT02394707
CMKLR1 va. 2	QuantiTect Primer Assay Hs_CMKLR1_2_SG	QT01680140
CXCR1	QuantiTect Primer Assay Hs_CXCR1_1_SG	QT00212919
CXCR2	QuantiTect Primer Assay Hs_CXCR2_1_SG	QT00000518
GPR1	QuantiTect Primer Assay Hs_GPR1_1_SG	QT00209748
RARRES2	QuantiTect Primer Assay Hs_RARRES2_1_SG	QT00091945

Supplementary Table S3: List of siRNAs used for the knockdown of Chemerin (RARRES 2 gene) purchased from qiagen company

Label	CAT No.	Target Sequence
RARRES2 siRNA 1	SI00045318	CTGGAAGAAACCCGAGTGCAA
RARRES2 siRNA 2	SI00045325	CCCAATGGGAGGAAACGGAAA
RARRES2 siRNA 5	SI03094469	CTGCATCAAACTGGGCTCTGA
RARRES2 siRNA 6	SI03102127	GACGGCCAGGGTGACACGGAA
Scrambled Control	1027280	(AllStars Negative Control)

Supplementary Table S4: List of shRNAs used for CCRL2 and GPR1 receptor knockdown in SCL-1 cells purchased from Genecoepia (Rockville, MD, USA)

Label	Product Name	Target Gene	Accession No.	Reporter Gene	Target Sequence
CCRL2 shRNA 1	HSH021922-1-LVRH1GP(CS9OS397048)	CCRL2	NM_003965.4	eGFP	GCAGAGCAATGTGACAAGTAT
CCRL2 shRNA 2	HSH021922-2-LVRH1GP(CS9OS397049)	CCRL2	NM_003965.4	eGFP	GCATCATTACAAGTGTCCTGG
CCRL2 shRNA 3	HSH021922-3-LVRH1GP(CS9OS397050)	CCRL2	NM_003965.4	eGFP	GACCAGAAATACAAGTGTGCA
CCRL2 shRNA 4	HSH021922-4-LVRH1GP(CS9OS397051)	CCRL2	NM_003965.4	eGFP	GCAAATACCTCTGCCGCTGTT
CCRL2 Scrambled Control	CSHCTR001-1-LVRH1GP(OSNEG20)	-	-	eGFP	GCTTCGCGCCGTAGTCTTA
GPR1 shRNA 5	HSH007828-5-LVRH1MP(OS397976)	GPR1	NM_005279.3	mCherry	GCTACTTGTGTCTCATCTTCA
GPR1 shRNA 5	HSH007828-6-LVRH1MP(OS397977)	GPR1	NM_005279.3	mCherry	GCTGGACTCCTTATCACCTGT
GPR1 shRNA 5	HSH007828-7-LVRH1MP(OS397978)	GPR1	NM_005279.3	mCherry	GCTCACCATTCACCACAATAG
GPR1 shRNA 5	HSH007828-8-LVRH1MP(OS397979)	GPR1	NM_005279.3	mCherry	GGTCCTCAGTTGCTGAGATAC
GPR1 Scrambled Control	CSHCTR001-1-LVRH1MP(OSNEG20)	-	-	mCherry	GCTTCGCGCCGTAGTCTTA